Chemistry & Biology
Brief Communication

Acyl-CoA Subunit Selectivity in the Pikromycin Polyketide Synthase PikAIV: Steady-State Kinetics and Active-Site Occupancy Analysis by FTICR-MS

Shilah A. Bonnett,[1,5] Christopher M. Rath,[2,5] Abdur-Rafay Shareef,[2] Joanna R. Joels,[2] Joseph A. Chemler,[2] Kristina Håkansson,[3] Kevin Reynolds,[1,*] and David H. Sherman[2,3,4,*]
[1]Department of Chemistry, Portland State University, Portland, OR 97201, USA
[2]Life Sciences Institute
[3]Department of Chemistry
[4]Department of Medicinal Chemistry and Department of Microbiology and Immunology
University of Michigan, Ann Arbor, MI 48104, USA
[5]These authors contributed equally to this work
*Correspondence: reynoldsk@pdx.edu (K.R.), davidhs@umich.edu (D.H.S.)
DOI 10.1016/j.chembiol.2011.07.016

SUMMARY

Polyketide natural products generated by type I modular polyketide synthases (PKSs) are vital components in our drug repertoire. To reprogram these biosynthetic assembly lines, we must first understand the steps that occur within the modular "black boxes." Herein, key steps of acyl-CoA extender unit selection are explored by in vitro biochemical analysis of the PikAIV PKS model system. Two complementary approaches are employed: a fluorescent-probe assay for steady-state kinetic analysis, and Fourier Transform Ion Cyclotron Resonance-mass spectrometry (FTICR-MS) to monitor active-site occupancy. Findings from five enzyme variants and four model substrates have enabled a model to be proposed involving catalysis based upon acyl-CoA substrate loading followed by differential rates of hydrolysis. These efforts suggest a strategy for future pathway engineering efforts using unnatural extender units with slow rates of hydrolytic off-loading from the acyltransferase domain.

INTRODUCTION

Polyketides are a structurally diverse class of natural products that function as antifungals (amphotericin B), immunosuppressives (FK506), antibiotics (erythromycin A) and other important pharmaceuticals (Walsh, 2004). The medicinal value of these compounds has inspired efforts to design novel molecules by reprogramming the polyketide synthase (PKS) pathways responsible for their assembly. Toward this end, it is crucial that we develop a deeper understanding of the chemical processes encoded by these systems (Wu et al., 2002). One current gap in our knowledge of modular PKSs is the mechanistic basis for substrate processing and discrimination toward acyl-coenzyme A (CoA) extender units (Figure 1, steps I–II).

Previous investigations have led to the proposal that acyltransferase (AT)-bound extender units are stable in modular PKSs and related fatty acid synthase (FAS) systems, with deacylation occurring only in the presence of a specific thiol acceptor (e.g., CoA or pantetheine) (Serre et al., 2005; Smith and Tsai, 2007; Tang et al., 2006, 2007). However, in the 6-deoxyerythronolide B synthase (DEBS) PKS, modules act as methylmalonyl-CoA (MM-CoA) hydrolases based on loss of radioactivity from [1-^{14}C]-MM-CoA (1)-labeled proteins (Marsden et al., 1994; Roberts et al., 1993). Thus, in the absence of a chain elongation intermediate, the extender unit may be hydrolytically released from the protein as methylmalonate (MM). Similar mechanisms have been proposed in FAS systems (Cognet and Hammes, 1983; Yuan and Hammes, 1985). Fundamental aspects of this process including the specific site and rates of hydrolysis, catalytic domains involved, and the molecular basis for acyl-CoA extender unit selectivity have not been reported.

In the current study, we investigated the fate of the acyl-CoA extender unit (Figure 1, steps I–II) and the role of the four catalytic domains (KS-AT-ACP-TE) of PikAIV (pikromycin (Pik) PKS module 6). Two complementary assays enabled us to probe this system including (1) a fluorescent assay using ThioGlo-1 to monitor the steady-state kinetics of extender unit uptake/free-CoA release, and (2) a Fourier Transform Ion Cyclotron Resonance Mass Spectrometry (FTICR-MS) method for directly monitoring active-site occupancy. Covalently linked intermediates at the KS (C207), AT (S652), ACP (S980 holo), and TE (S1196) were assessed by FTICR-MS with the data leading to a new mechanistic hypothesis for acyl-CoA processing. These assays are complementary in that the steady-state kinetic data provide a direct readout of catalysis in the system by monitoring substrate utilization, while the FTICR-MS assay rigorously interrogates the chemical occupancy of the enzymatic machinery (Dorrestein and Kelleher, 2006; Gu et al., 2007; Schnarr et al., 2005).

Four extender units were utilized in our analysis, including native MM-CoA, malonyl-CoA (M-CoA), propionyl-CoA (P-CoA), and ethylmalonyl-CoA (EM-CoA). The use of specific PKS variants in addition to the holo (phosphopantetheinylated) wild-type (WT) PikAIV (S980 holo), including: dKS (C207A/S980 holo),

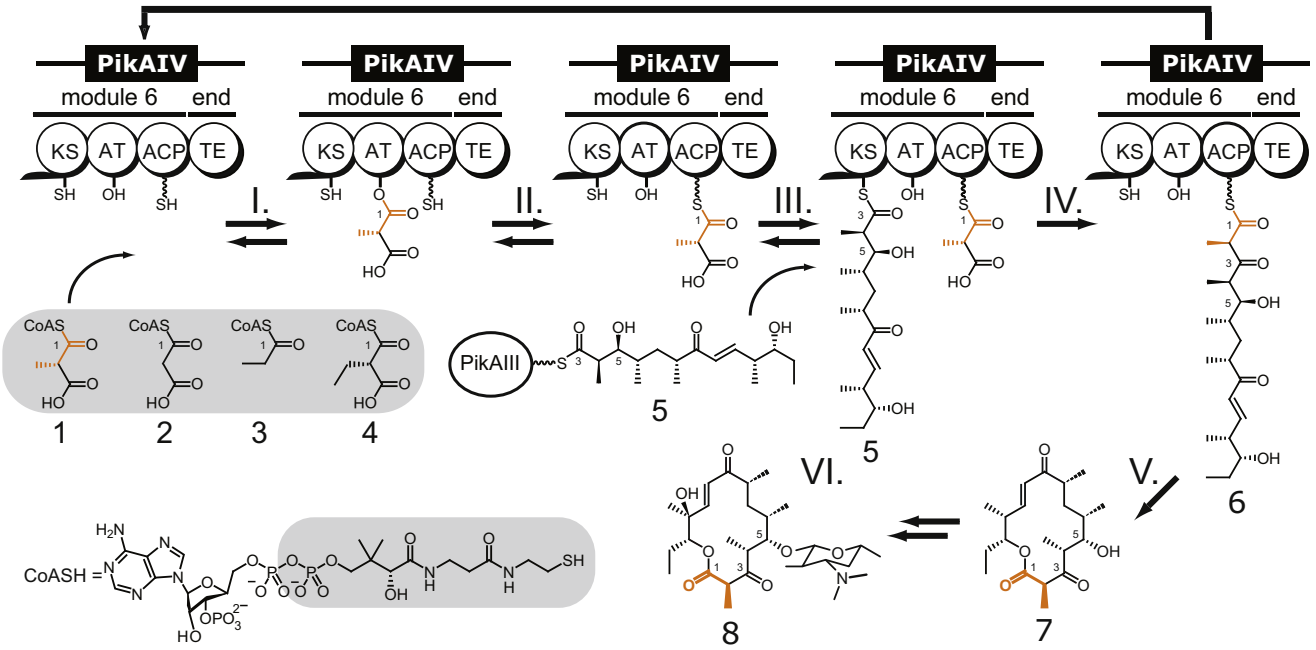

Figure 1. Catalytic Cycle for PikAIV

Acyl-CoA extender units (**1** native, **2-4** unnatural) are loaded onto the AT active-site serine as esters (step I) and undergo transfer to the ACP phosphopantetheine producing thioesters (gray portion of CoAS, step II). The hexaketide chain elongation intermediate (**5**) condenses with the MM-CoA extender unit (steps III-IV) to form the heptaketide (**6**) on the ACP prior to TE cyclization (Akey et al., 2006) to form narbonolide (**7,** step V) processed to pikromycin (**8,** step VI, Li et al., 2009) Reversible steps are noted by a backward arrow. Off-pathway reactions (e.g., hydrolysis from the active-site residues) are not illustrated.

dAT (S652A/S980 holo), apo (S980 apo) dTE (S1196A/S980 holo), and apo/dTE (S980 apo/S1196A) enabled us to assess the importance of individual domains in extender unit processing and hydrolytic activity (Kittendorf et al., 2007).

RESULTS AND DISCUSSION

In our PikAIV functional assay, loading of MM-CoA (Figure 1, step 1) was very rapid compared with hydrolysis (Table 1) or 10-deoxymethynolide production (3.3 ± 0.4 min^{-1}) (Aldrich et al., 2005). Rates were directly monitored as loss of free AT (S652) active-site hydroxyl (35 ± 23 s^{-1}) and the buildup of AT (S652) active-site bearing MM (21 ± 11 s^{-1}) (Figure S4/5) by rapid-quench and FTICR-MS (McLoughlin and Kelleher, 2004). Observed rates were similar to values reported for mammalian FAS-AT reactions with radiolabeled substrates (43-150 s^{-1}) (Cognet and Hammes, 1983; Yuan and Hammes, 1985).

The rates of MM-CoA hydrolysis (Table 1) were determined for the PikAIV variants under steady-state conditions in the absence of chain elongation intermediates with the ThioGlo-1 assay (Figure 1, steps I-II only, loading of extender unit with hydrolysis from active sites, Aldrich et al., 2005). Values were determined under identical in vitro biochemical conditions compared to previous analysis of the PikAIV system (Kittendorf et al., 2007). Holo PikAIV and the dKS (C207A) variant had the highest k_{cat} values (the dKS mutant had a slightly higher value, potentially due to increased access to the ACP bound thioester by water when docked in the KS active site). When the AT was inactivated (dAT, S652A) all hydrolytic activity was abolished. Inactivation of the ACP (S980 apo) or the dTE (S1196A) resulted in a cumulative effect for the apo-ACP/dTE (S980 apo/S1196A).

The analysis above revealed that the AT domain was the major site of hydrolysis accounting for ~70%–80% of activity. The ACP and TE domains are responsible for the remaining 20%–30% of the observed extender unit hydrolysis activity. MM is released as the free acid since the rate of triketide lactone formation from CoA extender units in PikAIV (0.00005-0.0001 min^{-1}) is substantially slower than the rate of hydrolysis determined in this study (Table 1) (Beck et al., 2003).

PikAIV active-site occupancy was determined by FTICR-MS under identical conditions to the ThioGlo-1 steady-state kinetic analysis (Table 2) (Aldrich et al., 2005). The KS active-site (C207) was not loaded for any PikAIV variants. The AT active-site S652 was saturated (AT:100%) when active, and no downstream loading of the ACP or TE occurred in the dAT (S652A) variant form of PikAIV. Moderate loading on to the ACP (S980 holo) was seen with WT (ACP:64%) and dKS (ACP:51%, C207A), while more MM accumulated in the dTE (S1196A) variant (ACP:87%). In the apo ACP variant (S980 apo) the AT was saturated (AT:100%) with no downstream TE (S1196) loading observed.

The ThioGlo-1 steady-state kinetic analysis and MS active-site occupancy data for PikAIV support an in vitro biochemical model in the bacterial type I modular PKS where native extender unit MM-CoA is loaded onto the AT active-site (Figure 1, step I), with substantial hydrolysis occurring directly at this site.

Table 1. MM-CoA Extender Unit Hydrolysis Rates of PikAIV

PikAIV	$k_{cat}(min^{-1})$	% Decrease k_{cat}
WT	1.04 ± 0.08	0
dKS	1.18 ± 0.07	−13
dAT	NA	100
Apo	0.81 ± 0.08	21
dTE	0.80 ± 0.10	23
Apo/dTE	0.70 ± 0.01	32

Apparent k_{cat} was determined using Michaelis-Menton kinetics by ThioGlo-1 assay with four replicates to calculate the standard deviation. Example data are illustrated in Figure S3.

Table 2. Extender Unit Active-Site Occupancy Analysis by FTICR-MS with Enzyme Variants and Alternative Substrates

PikAIV	Substrate	KS%	AT%	ACP%	TE%
WT	MM-CoA	0 ± 0	100 ± 0	64 ± 19	4 ± 0
dKS	MM-CoA	X	100 ± 0	51 ± 9	1 ± 0
dAT	MM-CoA	0 ± 0	X	0 ± 0	0 ± 0
Apo	MM-CoA	0 ± 0	100 ± 0	X	0 ± 0
dTE	MM-CoA	0 ± 0	100 ± 0	87 ± 13	X
Apo/dTE	MM-CoA	0 ± 0	100 ± 1	X	X
WT	M-CoA	0 ± 0	0 ± 0	3 ± 5	1 ± 0
WT	P-CoA	0 ± 0	0 ± 0	19 ± 13	0 ± 0
WT	EM-CoA	0 ± 0	90 ± 10	52 ± 46	6 ± 2

Percentages are the apparent active-site loading by comparing free active-site and covalent +MM active-site peptides. Four replicates were run to calculate %RSD. Figure S6 and Table S2 provide further information.

AT-bound MM is also transferred to the ACP (Figure 2, step II) and TE active-site, where further hydrolysis occurs.

The ability of PikAIV to select different acyl-CoA extender units (Figure 1, 1-4) was monitored by active-site occupancy using FTICR-MS (Table 2). For all species, no significant loading was observed on the KS active-site (C207). For the disfavored (based on predicted AT-domain specificity/observed product formation) M-CoA substrate, no loading on the AT domain (S652) was detected (Haydock et al., 1995). Low amounts of loading were also observed on the ACP (ACP:3%, S980 holo) and TE (TE:1% S1196) active-sites. Similarly, for the "dead-end" non-extendable P-CoA substrate, loading onto the AT active-site (S652) was not detected, but low levels were observed on the ACP (ACP:19%, S980 holo). For EM-CoA, which is a rare extender unit in PKS biosynthesis, a high level of loading onto the PikAIV AT (AT:90%, S652), ACP (ACP:52%, 980 holo), and TE (TE: 6%, S1196) active-sites was evident by FTICR-MS.

This occupancy data with M-CoA and P-CoA demonstrated that alternate extender units can be loaded onto an AT and transferred to the adjacent ACP. The high level AT loading with MM-CoA and EM-CoA led us to reason that a level of selectivity may be realized through hydrolytic activity of the disfavored substrate from the AT and ACP active sites.

To test this hypothesis, hydrolysis was monitored by the ThioGlo-1 steady-state assay (see Table S1 available online). When incubated in the presence of MM-CoA a baseline rate of hydrolysis was observed for holo PikAIV (WT), with a 27% lower rate for the apo variant, consistent with the role of the ACP and TE in facilitating hydrolysis (Table S1). For holo PikAIV (WT), a 5-fold increase in the rate of hydrolysis occurs upon substitution with M-CoA, due to acylation and subsequent deacylation with this non-preferred extender unit. For apo PikAIV a 10-fold increase in hydrolysis was observed with M-CoA. Thus, in the case of M-CoA loaded PikAIV, slow transfer to the ACP domain could contribute to the attenuated rate of M-CoA hydrolysis observed for the holo compared to apo. Overall, these data support the hypothesis that substrate discrimination against malonyl-CoA is mediated by subunit loading followed by hydrolysis at the AT domain. If the substrate were not loaded, then the rate of enzyme-catalyzed hydrolysis would be negligible.

The ability of PikAIV to select the correct extender unit from a mixture was tested by employing equimolar amounts of M-CoA and MM-CoA (Table S1). The observed total rate for this mixture was substantially closer to that observed for MM-CoA alone with the ThioGlo-1 assay. Only MM-loaded active-site residues were detected by FTICR-MS in this competition experiment (data not shown). Thus, in the presence of MM-CoA the futile turnover of M-CoA may be reduced due to the comparatively slow rate of MM hydrolysis from the saturated PikAIV AT active site.

Studies on the nonextendable P-CoA subunit offer additional insights into the function of PikAIV. Hydrolysis rates toward this subunit were found to be at an intermediate value between MM-CoA and M-CoA (Table S1). The PikAIV holo ACP species exhibited a faster hydrolytic rate than the corresponding apo protein. Whether P-CoA is loaded directly in vivo, or occurs from spontaneous decarboxylation of MM-CoA, it is likely that additional editing mechanisms have been developed to off-load this and other dead end intermediates (e.g., PikAV TEII, Kim et al., 2002).

The AT occupancy data for the EM-CoA (Table 2) are similar to MM-CoA, suggesting that there is slow hydrolysis of this extender unit. Indeed, neither the apo nor holo PikAIV variants resulted in detectable levels of hydrolytic activity of EM-CoA when analyzed in our ThioGlo-1 steady-state assay (Table S1). This suggests that relatively slow turnover (loading of extender unit and subsequent hydrolysis) is occurring with this extender unit. The ACP occupancy data indicated that PikAIV could accept EM-CoA as an alternate extender unit (see below). A lack of selectivity between EM-CoA and MM-CoA for AT units is not unexpected. A number of polyketide products, such as monensin, are generated in various analog forms using either MM-CoA or EM-CoA extender units at a specific point during chain elongation (Oliynyk et al., 2003; Liu and Reynolds, 1999). The EM and MM AT domain sequence motifs have a high degree of sequence similarity that have been predictive of AT acyl-CoA subunit selectivity in type I modular PKSs (Stassi et al., 1998; Suo et al., 2000). Moreover, it has been shown that an EM specific AT-domain substitution engineered into DEBS PKS module 5 can utilize MM-CoA (under limiting EM-CoA levels, Stassi et al., 1998; Suo et al., 2000). However, the observation that there is no significant hydrolysis of the EM-loaded PikAIV module is unexpected. A plausible hypothesis is that a relatively constrained AT active site allows hydrolysis of smaller extender units but not larger ones. High-resolution crystal structures with

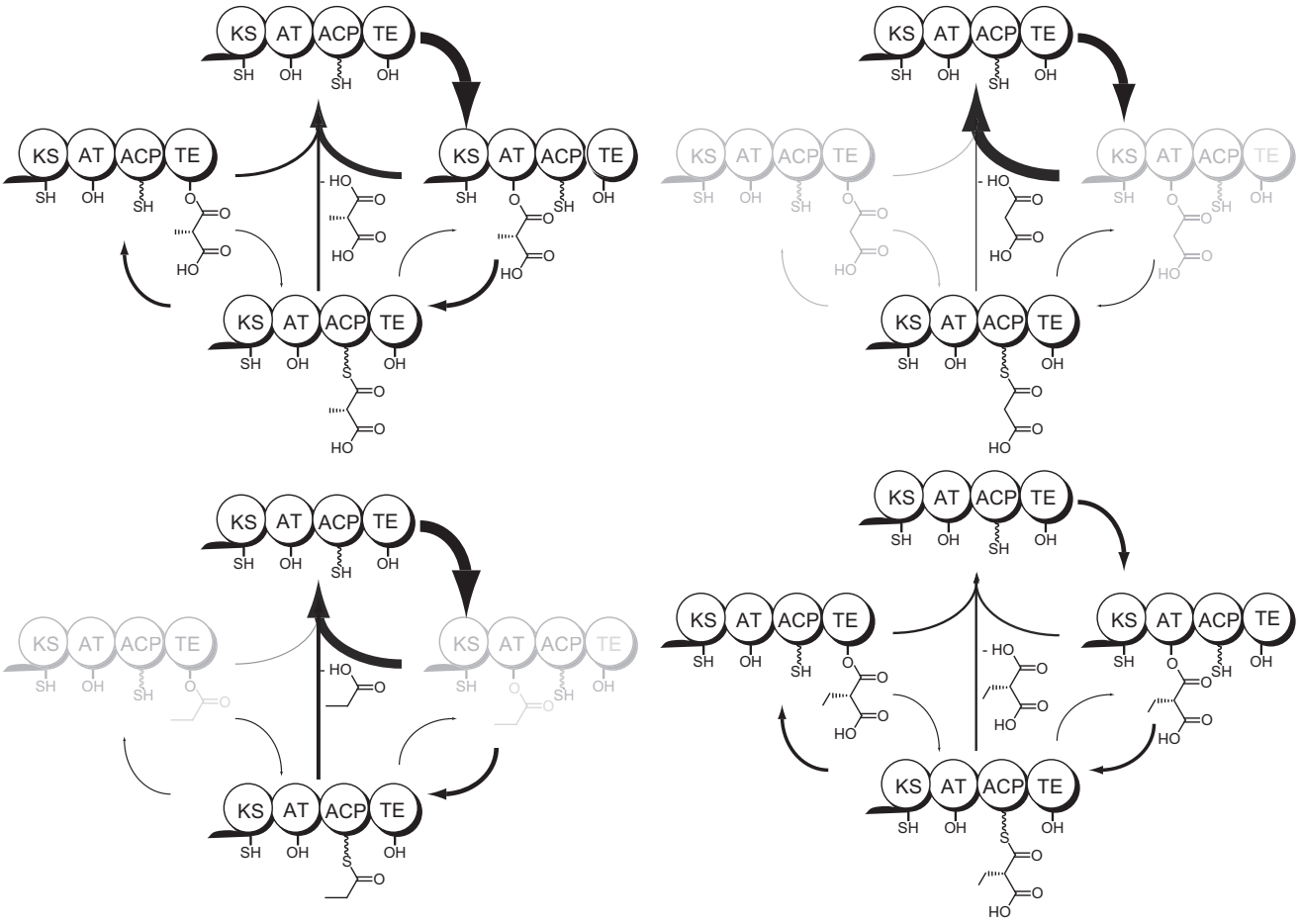

Figure 2. A Model for acyl-CoA Extender Unit Processing in the Terminal PikAIV PKS Module

Arrows represent proposed flux through the system based on ThioGlo-1 steady-state kinetic analysis. Presence/absence of intermediates, as indicated by black/gray coloration, was determined from FTICR-MS analysis of active-site occupancy.

modeled and/or bound substrates could be employed to test this possibility. Structural studies may provide further insight into the mechanistic basis for subunit hydrolysis in PKS AT domains.

The FT active-site occupancy and ThioGlo-1 steady-state acyl-CoA loading data enabled articulation of a new model for type I modular PKS biosynthesis based on the Pik system (Figure 2). For MM-CoA against PikAIV, loading occurs faster than hydrolysis, saturating the AT with transfer to the ACP and TE domains, which also contribute to hydrolysis (Figure 2A). For M-CoA, loading of this disfavored extender unit occurs, but it is rapidly removed by a high rate of hydrolysis. A small degree of M is transferred to the PikAIV ACP, competing with hydrolysis (Figure 2B). The dead-end P-CoA is similarly disfavored and is readily removed by hydrolysis (Figure 2C). In contrast, the unnatural substrate EM-CoA is loaded at PikAIV AT, ACP, and TE active sites and exhibits a slow rate of hydrolysis (Figure 2D).

The observation that PikAIV could effectively load the EM-CoA extender unit led us to investigate if the enzyme could produce the C2-ethyl narbonolide analog. This experiment serves as an example of how mechanistic insights (e.g., high levels of active-site loading with EM-CoA) can be applied to chemoenzymatic synthesis. The pikromycin SNAC-hexaketide chain elongation intermediate (Aldrich et al., 2005) was loaded onto PikAIV in the presence of EM-CoA. The reaction was extracted with organic solvent and product formation was monitored by LC FTICR-MS (Figure S7). The reaction of PikAIV, SNAC-hexaketide, and EM-CoA (Figure S7E) led to a new peak with the expected MH^+ of C2-ethyl narbonolide (5 ppm mass error). This peak has a similar elution profile compared to both the narbonolide authentic standard (Figure S7A), and chemoenzymatically generated narbonolide (Figure S7C). This product peak is absent in the no enzyme control reactions (Figures S7B and S7D). These data strongly suggest that in addition to successfully loading EM-CoA, PikAIV can also extend and cyclize it into a natural product. Thus, when engineering PKS pathways, the use of rare extender units lacking evolved selectivity may be a viable strategy to generate novel polyketide analogs. In a similar experiment using M-CoA as the extender unit, the corresponding C2-desmethyl narbonolide analog failed to be generated by PikAIV (data not shown), suggesting that acyl-CoA extender unit selectivity correlates with the ability to make the corresponding product.

SIGNIFICANCE

The results presented in this study have demonstrated that the PikAIV PKS (and presumably other PKS systems) contains an intrinsic acyl-CoA hydrolytic editing process. A unique insight from this investigation is that the initial acyl-CoA loading step occurs for extender units regardless of their ability to be incorporated into the natural product. Thus, final subunit occupancy is determined by reduced rates of hydrolysis in vitro (and presumably precursor pool levels in vivo), ultimately assuring proper acylation of the PKS module. Our ongoing analysis of other PKS monomodules, PikAIII and DEBS, has demonstrated similar hydrolytic activities and suggests a general metabolic process for AT subunit selectivity (unpublished data). Therefore, we may be able to exploit this characteristic by focusing on the use of unnatural extender units that undergo slow rates of hydrolysis. Efforts to tailor this hydrolytic activity, for example, by altering the active site of the KS-AT domains, could present new strategies for generating novel engineered natural products. As shown with EM-CoA, extender unit active-site occupancy and a slow rate of hydrolysis correlates with generation of a new macrocyclic natural product analog. Future efforts will focus on applying the complementary dual-assay system to effectively determine kinetic rates and other biochemical details, including polyketide subunit selection and β-keto group processing (Figure 1, steps 3 and 4), as well as docking domain interactions (Buchholz et al., 2009) and module → module transfer of chain elongation intermediates (McLoughlin and Kelleher, 2004). In principle, this dual-assay system is a powerful tool for exploring catalysis in PKS systems. Further verification of this in vitro model in other modular systems will help assess the generality of these findings. In the future, the FTICR-MS active-site analysis could be applied to directly extend this in vitro model toward investigation of biosynthesis of complex natural products in vivo.

EXPERIMENTAL PROCEDURES

Materials and General Methods

Unless otherwise noted, all chemicals, including acyl-CoAs, were purchased from Sigma. ThioGlo-1 [10-(2,5-dihydro-2,5-dioxo-1H-pyrrol-1-yl)-9-methoxy-3-oxo-methyl ester] was purchased either from Calbiochem or Covalent Associates. [1-^{14}C]-Malonyl-CoA was from Moravek. Hexaketide-SNAC was synthesized as previously described (Aldrich et al., 2005). Briefly, 10-deoxymethynolide was purified from a large-scale fermentation of *Streptomyces venezuelae* SC1016. After organic extraction and HPLC purification, 10-deoxymethynolide was reduced at the keto position and saponified with LiOH (seco-acid), followed by thioesterification to the activated (C7 reduced) SNAC hexaketide. Prior to enzymatic reactions, chemoselective allylic (MnO_2) oxidation and reverse phase HPLC purification yielded hexaketide as described below (Aldrich et al., 2005).

Cloning and Protein Expression

The construction of PikAIV mutants with KS, AT, and TE catalytic domains individually inactivated has been described previously (Kittendorf et al., 2007). The ACP domain was activated by expressing the protein in BAP1 cells to give the holo-form (Pfeifer et al., 2001). The ACP domain was inactivated (apo form) by expression in the presence of excess iron, thus inhibiting a promiscuous phosphopantetheinoyl transferase enzyme in *Escherichia coli*. Expression and purification of each of the PikAIV mutant proteins was achieved according to procedures described elsewhere (Kittendorf et al., 2007) and the resulting recombinant proteins were purified to >90% homogeneity as determined by SDS-PAGE (Figure S1). Protein concentrations were determined by the Quant-iT Assay kit (Invitrogen) or the BCA assay (Pierce) with BSA as a standard. Cloning and expression of the PikAIV KS-AT construct has been previously reported (Buchholz et al., 2009). The protein was overexpressed and purified using standard Ni-NTA chromatography (Figure S3).

For transient kinetic analysis, an internal standard peptide (IS) was generated through overexpression of a fusion construct. Briefly, the DNA encoding the PikAIV active-site peptide VWQHHGITPEAVIGHSQGEIAAAYVAGALTLD DAARSK was amplified from the plasmid containing PikAIV with Phusion DNA polymerase. This DNA was then cloned into the vector pMCSG7-MOCR with LIC technology. pMCSG7-MOCR is a variant of pMCSG7 with the protein MOCR (Walkinshaw et al., 2002) in frame (NCBI PT703G, courtesy Clay Brown LSI) and upstream of the LIC cloning/TEV cleavage site. A fusion partner was utilized, as the PikAIV ATIS peptide did not overexpress to a suitable level, potentially due to proteolysis. The MOCR-ATIS protein was then purified by standard Ni-NTA methodology, prior to TEV cleavage. The ATIS peptide could be purified from MOCR and TEV by RP-HPLC using a 4000A PLRP-S column and a gradient of 0%–100% 0.1% formic acid and acetonitrile + 0.1% formic acid (Figure S2). Fractions containing the ATIS were collected, and concentration was determined by the BCA assay. The ATIS was also characterized by MS/MS as described below. The final PikAIV ATIS peptide contains three additional residues from the TEV cleavage site for a sequence of: SNAVWQHHGITPEAVIGHSQGEIAAAYVAGALTLDDAARSK.

The *S. collinus ccr* gene was excised as a 1.3 kb NdeI-HindIII fragment from pHL18 (Liu and Reynolds, 1999) and subcloned into pET28a to produce pCH1, which was used to transform *E. coli* BL21(DE3). The resulting transformant was used to inoculate 200 ml of LB medium supplemented with 50 μg/ml of kanamycin, grown at 37°C to an optical density (OD_{600}) of 0.7, induced with 0.1 mM IPTG, and grown for a further 3 hr. CCR was purified by Ni-affinity chromatography (according to standard protocols) and dialyzed against 50 mM Tris-HCl (pH 7.2). Ethylmalonyl-CoA was produced by incubation of 1 μM CCR, 15 mM crotonyl-CoA, 16 mM NADPH, and 200 mM $NaHCO_3$ in 50 mM Tris-HCl (pH 7.5). Reaction progress was assessed spectrophotometrically at 340 nm.

Kinetic Analysis of Hydrolytic Activity

All reactions were carried out at 30°C in the presence of 400 mM sodium phosphate (pH 7.2), 5 mM NaCl, 20% glycerol, 0.5 mM TCEP, varying concentration of methylmalonyl-CoA and either 0.5 or 1 μM of protein. A series of controls were conducted in parallel, including the use of boiled protein, to ensure hydrolysis of acyl-CoAs was due to enzymatic activity. Aliquots (50 μl) were withdrawn at specific time points and added to a well of a black 96-well plate containing an equal volume of dimethyl sulfoxide (DMSO) to quench the reaction. 100 μl of a 200 μM ThioGlo-1 solution (in DMSO) was added to each well, and the plate was incubated in the dark at room temperature with gentle shaking for 20 min. All samples were analyzed by fluorescence (excitation 378 nm and emissions at 480 nm) using a Gemini XPS microplate spectrofluorometer (Molecular Devices). The relative fluorescent unit (RFU) was converted to concentration using a standard CoA curve. Kinetic parameters were calculated from the average of at least three sets of triplicates with the Michaelis-Menten equation using the curve fitting software Kaleidagraph 4.03 (Synergy Software, Reading, PA) (Figure S3).

Substrate Specificity and Competition Assays

The hydrolytic activity of WT, apo and dAT PikAIV proteins were examined in the presence of 1 mM malonyl-CoA or 1 mM ethylmalonyl-CoA under conditions described above. Aliquots (25 μl) were withdrawn at specific time points and added to a well of a black 96 well plate containing 75 μl of DMSO to quench the reaction. 100 μl of a 200 μM ThioGlo1 solution (in DMSO) was added to each well, and the plate was incubated in the dark at room temperature with gentle shaking for 20 min and analyzed by fluorescence as described above. For the competition assays, WT and apo PikAIV proteins were incubated in the presence of 1 mM methylmalonyl-CoA and 1 mM malonyl-CoA.

FTICR-MS Analysis of Active-Site Occupancy

PikAIV (1 μM) was reacted with acyl-CoA extender units under saturating conditions (1 mM) in the presence of 400 mM sodium phosphate (pH 7.2),

5 mM NaCl, 20% glycerol, and 1 mM TCEP. Reactions were incubated at 25°C for 10 min, followed by a 2.5 fold dilution in 50 mM ammonium bicarbonate with tris-base added (pH 8). Trypsin was present at an enzyme to substrate ratio of 1:10. Proteolysis was allowed to proceed for 15 min at 37°C followed by addition of formic acid (pH 4). Thirty and 45 min digests yielded similar results, suggesting that hydrolysis from the active-site peptides is insignificant compared with other sources of experimental error. Reactions were frozen at −20°C until analysis. Fifty microliters of sample (20 pmol/3 μg of protein) was injected onto a Jupiter C4 2 × 250 mm 300 μm column (Phenomenex) using an Agilent 1100 LC system with a flow rate of 200 μl/min and a gradient of 2%–98% acetonitrile over 40 min. 0.1% formic acid was added to the water and acetonitrile solvents. A divert valve was utilized for online desalting. The LC was coupled to an FTICR-MS (APEX-Q with Apollo II ion source and actively shielded 7 T magnet; Bruker Daltonics). Data were gathered from m/z 200–2000 in positive ion mode. Electrospray was conducted at 2600 V with one scan per spectra utilizing 0.33 s external ion accumulation in a hexapole and 1 ICR cell fills prior to excitation and detection. Data were analyzed using DECON2LC (Pacific Northwest National Labs), VIPER (Pacific Northwest National Labs), and Data Analysis (Bruker Daltonics). Similar ionization efficiencies were assumed between the loaded and unloaded form, as no functional groups which either introduce or remove a charge site in positive mode ESI conditions (pH <3) are different between the loaded and unloaded forms. Changes in overall mass and hydrophobicity may have an impact, but on the relatively large peptides monitored this is likely less significant than other experimental variation in this semiquantitative method.

Transient Kinetic Analysis

PikAIV KS-AT didomain (2 μM) was mixed with an equal volume of acyl-CoA extender units (2 mM) in a Kintech rapid-quench apparatus equilibrated to 30°C for a 2-fold dilution. Each reagent was in the following buffer: 400 mM sodium phosphate (pH 7.2), 5 mM NaCl, 20% glycerol, and 1 mM TCEP. Data were recorded at time points 2, 4, 5, 8, 32, 64, and 128 ms in triplicate. Each reaction was immediately quenched in 1 M HCl in 6 M urea then heated for 3 min at 90°C. Each reaction was then frozen in liquid nitrogen. After all reactions were conducted, they were simultaneously thawed and diluted to 2 M urea in 50 mM ammonium bicarbonate, and the pH was adjusted to 8.0 with tris-base. Two microliters of Lys-C (Roche) was then added to each reaction for a final concentration of 0.2 mg/ml. The samples were then incubated for 15 min at 37°C after which the pH was reduced to 4.0 with 10% formic acid. Samples were desalted with Handee Microspin columns (Pierce) packed with 20 μl of 300 Å polymeric C18 resin (Vydac). Samples were loaded onto the columns and washed with 30 column volumes of 0.1% formic acid prior to elution with ten column volumes of 50% acetonitrile plus 0.1% formic acid. Intact protein samples were analyzed by FTICR-MS (APEX-Q with Apollo II ion source and actively shielded 7T magnet; Bruker Daltonics). Data were gathered from m/z 200–2000 utilizing direct infusion electrospray ionization in positive ion mode. Electrospray was conducted at 3600 V with 24 scans per spectra utilizing 1 s external ion accumulation in a hexapole and four ICR cell fills prior to excitation and detection. The external quadrapole was set to only allow ions from 740–815 m/z to reach the FTICR mass analyzer. Data were processed in Data Analysis (Bruker Daltonics) and Midas (NHMFL). All identified species were accurate to 20 ppm with external calibration. The PikAIV AT active site, and PikAIV AT MM loaded active site were quantified by total peak height for each isotope in comparison to the PikAIV AT active-site internal standard peptide, which was added at 2 μM during sample preparation. This peptide contains the additional three residues SNA- at the N terminus from the TEV cleavage site.

LC-FTICR-MS Analysis of Product Formation

Chain elongation unit and extender unit product formation was examined by LC-FTICR-MS and confirmed by LC-MS/MS. PikAIV (1 μM) was reacted with CoA extender units under saturating conditions (1 mM) and SNAC-hexaketide (1 mM) in the presence of 400 mM sodium phosphate (pH 7.2), 5 mM NaCl, 20% glycerol, 1 mM TCEP. The 100 μl reactions were incubated overnight at room temperature. Samples were extracted with chloroform (3:1 ratio) and concentrated under N_2. The sample was reconstituted in 200 μl of MeOH and 50 μl of this sample was analyzed on a Zorbax C8 300 Å 2 × 50 mm 5 μm column (Phenomenex). A gradient was generated on an Agilent 1100 HPLC. The following conditions were used 0 (90,10), 5 (90,10), 20 (2,98), 24 (2,98), and 25 (98,2). Values are provided as time (%A, %B) (minutes), with the total run time of 30 min. Flow was at 0.2 ml/min. A column heater was operated at 50°C. Flow was diverted for the first 5 min of the run. Buffer A consisted of 0.1% formic acid in DDI water. Buffer B consisted of 0.1% FA in acetonitrile.

FTICR-MS was performed on an APEX-Q (Apollo II ion source 7 T magnet, Bruker Daltonics). Data were gathered by ESI in positive ion mode (2400 V, m/z 150–1000, transient 128 K, 1 scan/spectrum) with external ion accumulation, dynamic trapping (0.33 s), and 1 ICR cell fill per spectrum. External calibration utilized HP-mix (Agilent). Product peaks were detected over multiple samples and runs.

SUPPLEMENTAL INFORMATION

Supplemental Information includes seven figures and two tables and can be found with this article online at doi:10.1016/j.chembiol.2011.07.016.

ACKNOWLEDGMENTS

This work was supported by NIH grant R01 GM076477 and the Hans W. Vahlteich Professorship (to D.H.S.).

Received: April 10, 2011
Revised: June 23, 2011
Accepted: July 4, 2011
Published: September 22, 2011

REFERENCES

Akey, D.L., Kittendorf, J.D., Giraldes, J.W., Fecik, R.A., Sherman, D.H., and Smith, J.L. (2006). Structural basis for macrolactonization by the pikromycin thioesterase. Nat. Chem. Biol. *2*, 537–542.

Aldrich, C.C., Beck, B.J., Fecik, R.A., and Sherman, D.H. (2005). Biochemical investigation of pikromycin biosynthesis employing native penta- and hexaketide chain elongation intermediates. J. Am. Chem. Soc. *127*, 8441–8452.

Beck, B.J., Aldrich, C.C., Fecik, R.A., Reynolds, K.A., and Sherman, D.H. (2003). Iterative chain elongation by a pikromycin monomodular polyketide synthase. J. Am. Chem. Soc. *125*, 4682–4683.

Buchholz, T.J., Geders, T.W., Bartley, F.E., 3rd, Reynolds, K.A., Smith, J.L., and Sherman, D.H. (2009). Structural basis for binding specificity between subclasses of modular polyketide synthase docking domains. ACS Chem. Biol. *4*, 41–52.

Cognet, J.A.H., and Hammes, G.G. (1983). Elementary steps in the reaction mechanism of chicken liver fatty acid synthase: acetylation-deacetylation. Biochemistry *22*, 3002–3007.

Dorrestein, P.C., and Kelleher, N.L. (2006). Dissecting non-ribosomal and polyketide biosynthetic machineries using electrospray ionization Fourier-Transform mass spectrometry. Nat. Prod. Rep. *23*, 893–918.

Gu, L., Geders, T.W., Wang, B., Gerwick, W.H., Håkansson, K., Smith, J.L., and Sherman, D.H. (2007). GNAT-like strategy for polyketide chain initiation. Science *318*, 970–974.

Haydock, S.F., Aparicio, J.F., Molnár, I., Schwecke, T., Khaw, L.E., König, A., Marsden, A.F.A., Galloway, I.S., Staunton, J., and Leadlay, P.F. (1995). Divergent sequence motifs correlated with the substrate specificity of (methyl)malonyl-CoA:acyl carrier protein transacylase domains in modular polyketide synthases. FEBS Lett. *374*, 246–248.

Kim, B.S., Cropp, T.A., Beck, B.J., Sherman, D.H., and Reynolds, K.A. (2002). Biochemical evidence for an editing role of thioesterase II in the biosynthesis of the polyketide pikromycin. J. Biol. Chem. *277*, 48028–48034.

Kittendorf, J.D., Beck, B.J., Buchholz, T.J., Seufert, W., and Sherman, D.H. (2007). Interrogating the molecular basis for multiple macrolactone ring formation by the pikromycin polyketide synthase. Chem. Biol. *14*, 944–954.

Li, S.J., Chaulagain, M.R., Knauff, A.R., Podust, L.M., Montgomery, J., and Sherman, D.H. (2009). Selective oxidation of carbolide C-H bonds by an engineered macrolide P450 mono-oxygenase. Proc. Natl. Acad. Sci. USA *106*, 18463–18468.

Liu, H., and Reynolds, K.A. (1999). Role of crotonyl coenzyme A reductase in determining the ratio of polyketides monensin A and monensin B produced by *Streptomyces cinnamonensis*. J. Bacteriol. *181*, 6806–6813.

Marsden, A.F., Caffrey, P., Aparicio, J.F., Loughran, M.S., Staunton, J., and Leadlay, P.F. (1994). Stereospecific acyl transfers on the erythromycin-producing polyketide synthase. Science *263*, 378–380.

McLoughlin, S.M., and Kelleher, N.L. (2004). Kinetic and regiospecific interrogation of covalent intermediates in the nonribosomal peptide synthesis of yersiniabactin. J. Am. Chem. Soc. *126*, 13265–13275.

Oliynyk, M., Stark, C.B.W., Bhatt, A., Jones, M.A., Hughes-Thomas, Z.A., Wilkinson, C., Oliynyk, Z., Demydchuk, Y., Staunton, J., and Leadlay, P.F. (2003). Analysis of the biosynthetic gene cluster for the polyether antibiotic monensin in *Streptomyces cinnamonensis* and evidence for the role of *monB* and *monC* genes in oxidative cyclization. Mol. Microbiol. *49*, 1179–1190.

Pfeifer, B.A., Admiraal, S.J., Gramajo, H., Cane, D.E., and Khosla, C. (2001). Biosynthesis of complex polyketides in a metabolically engineered strain of *E. coli*. Science *291*, 1790–1792.

Roberts, G.A., Staunton, J., and Leadlay, P.F. (1993). Heterologous expression in *Escherichia coli* of an intact multienzyme component of the erythromycin-producing polyketide synthase. Eur. J. Biochem. *214*, 305–311.

Schnarr, N.A., Chen, A.Y., Cane, D.E., and Khosla, C. (2005). Analysis of covalently bound polyketide intermediates on 6-deoxyerythronolide B synthase by tandem proteolysis-mass spectrometry. Biochemistry *44*, 11836–11842.

Serre, L., Verbree, E.C., Dauter, Z., Stuitje, A.R., and Derewenda, Z.S. (2005). The *Escherichia coli* malonyl-CoA: acyl carrier protein transacylase at 1.5Å-resolution. J. Biol. Chem. *270*, 12961–12964.

Smith, S., and Tsai, S.C. (2007). The type I fatty acid and polyketide synthases: a tale of two megasynthases. Nat. Prod. Rep. *24*, 1041–1072.

Suo, Z., Chen, H., and Walsh, C.T. (2000). Acyl-CoA hydrolysis by the high molecular weight protein 1 subunit of yersiniabactin synthetase: mutational evidence for a cascade of four acyl-enzyme intermediates during hydrolytic editing. Proc. Natl. Acad. Sci. USA *97*, 14188–14193.

Stassi, D.L., Kakavas, S.J., Reynolds, K.A., Gunawardana, G., Swanson, S., Zeidner, D., Jackson, M., Liu, H., Buko, A., and Katz, L. (1998). Ethyl-substituted erythromycin derivatives produced by directed metabolic engineering. Proc. Natl. Acad. Sci. USA *95*, 7305–7309.

Tang, Y., Kim, C.Y., Mathews, I.I., Cane, D.E., and Khosla. (2006). The 2.7-Å crystal structure of a 194-kDa homodimeric fragment of the 6-deoxyerythronolide B synthase. Proc. Natl. Acad. Sci. USA *69*, 11124–11129.

Tang, Y., Chen, A.Y., Kim, C.Y., Cane, D.E., and Khosla, C. (2007). Structural and mechanistic analysis of protein interactions in module 3 of the 6-deoxyerythronolide B synthase. Chem. Biol. *14*, 931–943.

Walkinshaw, M.D., Taylor, P., Sturrock, S.S., Atanasiu, C., Berge, T., Henderson, R.M., Edwardson, J.M., and Dryden, D.T.F. (2002). Structure of Ocr from bacteriophage T7, a protein that mimics B-form DNA. Mol. Cell *9*, 187–194.

Walsh, C.T. (2004). Polyketide and nonribosomal peptide antibiotics: modularity and versatility. Science *303*, 1805–1810.

Wu, N., Cane, D.E., and Khosla, C. (2002). Quantitative analysis of the relative contributions of donor acyl carrier proteins, acceptor ketosynthases, and linker regions to intermodular transfer of intermediates in hybrid polyketide synthases. Biochemistry *41*, 5056–5066.

Yuan, Z.Y., and Hammes, G.G. (1985). Elementary steps in the reaction mechanism of chicken liver fatty acid synthase. Acylation of specific binding sites. J. Biol. Chem. *260*, 13532–13538.